Письма в ЖЭТФ, том 55, вып.6, стр.358 - 362 25 марта 1992 г.

PHASE DIAGRAM OF COHERENTLY PRECESSING STATES UNDER SUPERFLOW IN ^{3}He-B

J.S. Korhonen[1)], *G.E. Volovik*[2),1)]

[1)] *Low Temperature Laboratory, Helsinki University of Technology, 02150, Espoo, Finland*
[2)] *Landau Institute for Theoretical Physics, 117334 Moscow, USSR*

Submitted 22 February 1992

The phase diagram for the ordered B-phase states under the condition of the transverse NMR is constructed. Three phases including the homogeneously precessing states are separated by the first order transition lines.

The coherent Larmor precession of magnetization in superfluid ^{3}He-B represents the time-dependent ordered state with the utmost broken symmetry in condensed matter. The precessing state has a rigidity, which is the main feature of the ordered state with broken symmetry. This provides the high stability of coherent precession. Such anomalously stable coherent precession of magnetization (homogeneously precessing domain, HPD) has been discovered in 1984 by the combined theoretical and experimental efforts,[1] and now serves for the experimental investigation of the intricate properties of the ^{3}He-B in presence of superflow.[2,3] These experiments require the detailed knowledge of the interaction of the precessing state with the vortex cluster and with the counterflow $\vec{v}_s - \vec{v}_n$ of the superfluid and normal components of the ^{3}He-B outside the cluster. The pioneering theoretical work on this subject has been made by Bunkov and Timofeevskaya [4], who investigated the structure of the domain boundary between the HPD and nonprecessing domain (NPD) in the presence of the counterflow.

Here we discuss the domain boundaries from the general arguments of the first order phase transition between different ordered states, which can exist in superfluid ^{3}He-B under conditions of the transverse NMR, i.e. when the small rf field with the frequency ω close to the Larmor frequency γH is applied perpendicular to the external field $\vec{H}$ (γ is the gyromagnetic ratio for ^{3}He nucleus, which we further put unity). We find the phase diagram between three ordered states, see Fig.1: (i) HPD, (ii) NPD and (iii) the precessing state with the direction of magnetization opposite to $\vec{H}$ (reversed spin domain, RSD). The first order phase transitions between these states provide the existence of three domain boundaries: HPD-NPD, HPD-RSD and NPD-RSD, which position in the vessel can be stabilized by application of the field or velocity gradient. The structure of the HPD-NPD phase boundary within the vortex cluster and in the presence of the counterflow is discussed.

The Larmor precession of ^{3}He-B in the limit case, when the dipole interaction is neglected, can be obtained from the initial stationary state with the equilibrium magnetization $\vec{S}^{(0)} = \chi\vec{H}$ and orthogonal order parameter matrix $\mathrm{R}^{(0)}$ by special symmetry operation, which comes from the Larmor theorem. According to Larmor theorem, the effect of magnetic field on the spins of the ^{3}He atoms completely disappears in the system rotating with the Larmor frequency. Therefore the spin rotation operation in the precessing frame does not change the energy of the system. If $\mathrm{R}^{(p)}$ is the matrix of spin rotations in the precessing frame, it defines the orientation of the B-phase order parameter matrix $R_{\alpha i}(t)$ and magnetization $S_\alpha(t)$ for the general Larmor precession in the following way:

$$R_{\alpha i}(t) = O_{\alpha\beta}(\hat{z}, \omega t) R^{(p)}_{\beta\gamma} O_{\gamma\mu}(\hat{z}, -\omega t) R^{(0)}_{\mu i}, \quad S_\alpha(t) = O_{\alpha\beta}(\hat{z}, \omega t) R^{(p)}_{\beta\gamma} S^{(0)}_\gamma \quad , \qquad (1)$$

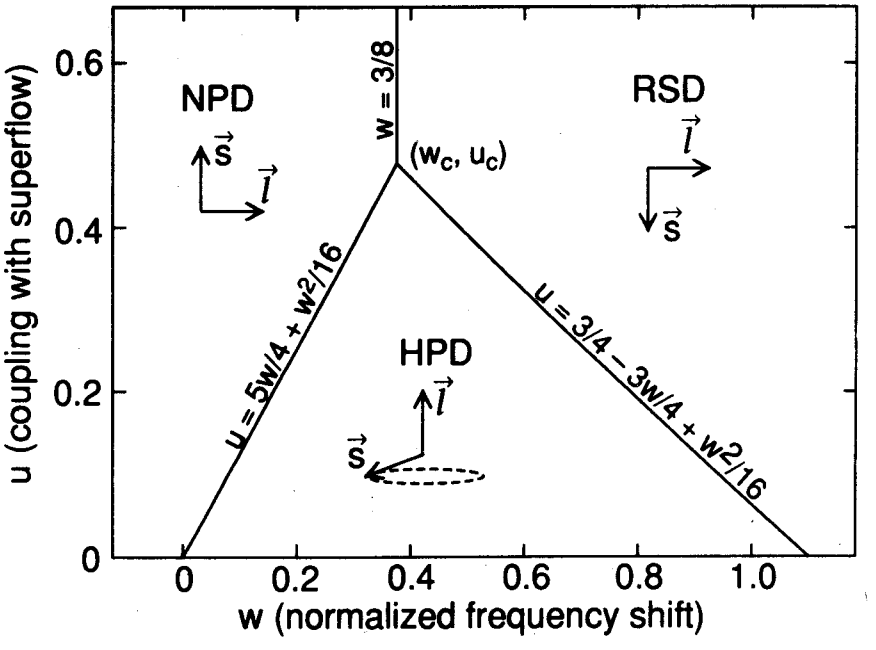

Fig.1. Phase diagram for the coherent states. The transitions are of the first order except the point $(u = 0, w = 0)$.

where $O(\hat{z}, \omega t)$ is the transformation from the laboratory frame into the rotating frame - this is the rotation about axis z (along $\vec{H}$) by angle ωt. The Eq.(1) means that to produce the symmetry transformation one should first make the transformation from the laboratory frame into the precessing frame, then produce the $R^{(p)}$ rotation within this frame and after that return back to the laboratory frame.

The space of the degenerate states of the Larmor precession is larger than in the stationary state: in addition to the degeneracy parameter $R^{(0)}$ the Larmor precession is characterised also by another time independent matrix $R^{(p)}$. The physical meaning of these matrices is as follows: the $R^{(p)}$ matrix shows the orientation of the spin in the precessing frame according to Eq.(1), $S_\beta^{(p)} = R_{\beta\gamma}^{(p)} S_\gamma^{(0)}$. If $\hat{s}$ is the direction of the magnetization in the precessing frame, then its projection on $\vec{H}$ is $\hat{s}_z = R_{zz}^{(p)}$. The $R^{(0)}$ matrix shows the orientation $\vec{l}$ of the orbital momentum $L_i = -R_{\alpha i}(t) S_\alpha(t) = -R_{\alpha i}^{(0)} S_\alpha^{(0)}$, which is constant in the laboratory frame. If $\hat{l}_z$ is the z projection of $-\vec{l}$, one has $\hat{l}_z = R_{zz}^{(0)}$.

Three terms contribute the energy of the coherently precessing state and lift the degeneracy. (i) The dipole energy after averaging over the period of precession depends on only three degeneracy parameters:

$$F_D = \frac{2}{15}\chi\Omega_L^2[(\hat{s}_z\hat{l}_z - \frac{1}{2} + \frac{1}{2}\cos\gamma(1+\hat{s}_z)(1+\hat{l}_z))^2 +$$

$$\frac{1}{8}(1-\hat{s}_z)^2(1-\hat{l}_z)^2 + (1-\hat{s}_z^2)(1-\hat{l}_z^2)(1+\cos\gamma)] \quad . \qquad (2)$$

Here Ω_L is the Leggett frequency, and if one introduces the Euler angles for matrices $R = R_z(\alpha)R_y(\beta)R_z(\gamma)$, then $\gamma = \gamma^{(p)} - \gamma^{(0)}$. Note the symmetry between the spin and orbital vectors $\hat{s}$ and $-\hat{l}$ in the dipole energy.

(ii) The so-called spectroscopic term appears if the frequency of the rf field deviates from Larmor frequency. In this case the Zeemann energy $-\vec{H}\cdot\vec{S}$ is not compensated completely by the Larmor energy of precession $\vec{\omega}\cdot\vec{S}$, therefore one

has the difference

$$F_\omega = (\vec{\omega} - \vec{H}) \cdot \vec{S} = \chi\omega(\omega - H)\hat{s}_z \quad . \tag{3}$$

(iii) Typically under rotation of the vessel the vortex cluster appears at the center of the vessel, separated by the vortex-free counterflow region from the side walls. Vortices and counterflow interact with the orbital anisotropy vector $\hat{l}$:[5]

$$F_{\text{counterflow}} = -\frac{1}{2}\rho_a((\vec{v}_s - \vec{v}_n) \cdot \hat{l})^2 \quad , \quad F_{\text{vortices}} = \lambda_{\text{vortices}}(\hat{\Omega} \cdot \hat{l})^2 \quad , \tag{4}$$

where $\hat{\Omega}$ is the direction of rotation.

The equilibrium states are obtained by the minimization of $F = F_D + F_\omega + F_{\text{vortices}}$ within the vortex cluster or $F = F_D + F_\omega + F_{\text{counterflow}}$ within the counterflow region. If $\hat{\Omega} \parallel \vec{H}$ both energies have the same structure:

$$\tilde{F} = u\hat{l}_z^2 + v\hat{s}_z + [(\hat{s}_z\hat{l}_z - \frac{1}{2} + \frac{1}{2}\cos\gamma(1 + \hat{s}_z)(1 + \hat{l}_z))^2 +$$

$$\frac{1}{8}(1 - \hat{s}_z)^2(1 - \hat{l}_z)^2 + (1 - \hat{s}_z^2)(1 - \hat{l}_z^2)(1 + \cos\gamma)] \quad , \tag{5}$$

where we normalized the energy in terms of the dipole energy introducing the dimensionless variables:

$$\tilde{F} = \frac{15F}{2\chi\Omega_L^2} \quad , \quad w = \frac{15\omega(\omega - H)}{2\Omega_L^2} \quad , \quad u = \frac{15\rho_a(\vec{v}_s - \vec{v}_n)^2}{4\chi\Omega_L^2} \quad \text{or} \quad u = \frac{15\lambda_{\text{vortices}}}{2\chi\Omega_L^2} \quad . \tag{6}$$

Minimization shows that there are three competing states: (i) Nonprecessing state (NPD) with $\hat{s}_z = 1$, $\hat{l}_z = 0$ and $\cos\gamma = 1/2$; (ii) HPD with $\hat{l}_z = 1$ and $\cos\gamma = 1$, the precessing magnetization is tilted by angle $\cos\beta = \hat{s}_z = -\frac{1}{4} - \frac{w}{8}$; and (iii) the precessing state with the reversed spin (RSD): $\hat{s}_z = -1$, $\hat{l}_z = 0$, while γ is arbitrary. This state differs from the periodic solution with $\hat{s}_z = -1$ discussed by Fomin[6] by orientation of $\hat{l}$, and therefore has different stability condition. The energies of these states are

$$\tilde{F}_{\text{NPD}} = w \quad , \quad \tilde{F}_{\text{HPD}} = u - \frac{1}{4}w - \frac{1}{16}w^2 \quad , \quad \tilde{F}_{\text{RSD}} = -w + \frac{3}{4} \quad , \tag{7}$$

and the phase diagram in w, u plane contains the triple point $w_c = \frac{3}{8}$, $u_c = \frac{489}{1024}$ where three first order transition lines merge together (see Fig. 1).

The transition line between HPD and NPD, at which $F_{\text{HPD}} = F_{\text{NPD}}$,

$$u = \frac{5}{4}w + \frac{1}{16}w^2 \quad , \tag{8}$$

represents the first order phase transition except the point $w = 0$, $u = 0$. The first order transition line between RSD and NPD, $w = \frac{3}{8}$, exists at $u > u_c$. The first order transition line between HPD and RSD, $u = \frac{3}{4} - \frac{3}{4}w + \frac{1}{16}w^2$, exists at $u < u_c$, $w > w_c$ and gives rise to the domain boundary between HPD and RSD (Fig. 2). Due to the first order nature of the phase transitions the metastability is possible. The HPD state is metastable in the regions of the NPD or RSD stability until it becomes absolutely unstable at $u = \frac{15}{8} - \frac{3}{32}w - \frac{5}{64}w^2$. Above this line the instability towards the deviation of $\hat{l}$ from the $\hat{z}$ direction develops. The instability of the NPD towards RSD develops at $w > 3$, it starts with the deviation of $\hat{s}$ from the $\hat{z}$ direction. The instability of RSD towards NPD develops at $w < 0$. We also found another metastable local minimum of Eq.(5) with $\hat{l}_z = -1$ and $\hat{s}_z = -\frac{w}{3}$.

Now let us consider the core structure of the domain boundary between HPD and NPD. The simplest structure is obtained in the limit of the infinitely large

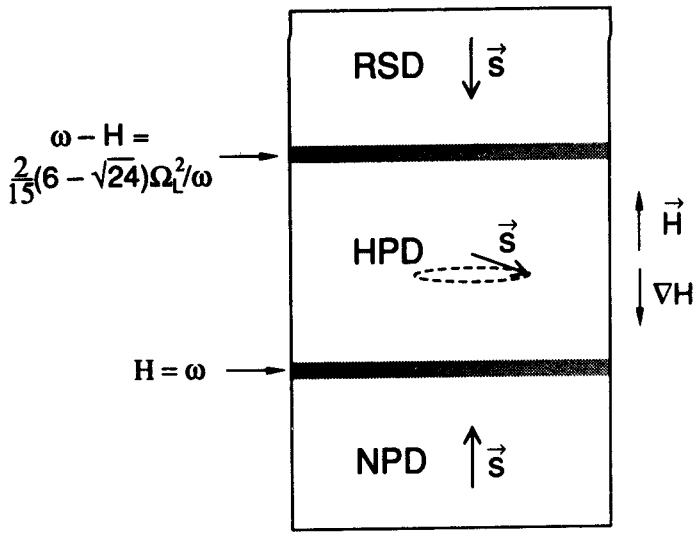

Fig.2. Three-domains precession under large field gradient along z; $0 \le u < u_c$. In the absence of the counterflow ($u = 0$) the positions z_1 and z_2 of the domain boundaries are defined by $H(z_1) = \omega$ for HPD-NPD boundary and $\omega - H(z_2) = \frac{2}{15}(6-\sqrt{24})\frac{\Omega_L^2}{\omega}$ for the HPD-RSD boundary.

dipole energy, compared to the interaction with the counterflow or with the vortex cluster. From minimization of Eq.(2) only it follows that at each point of space, including the core of the domain boundary, one has either $\hat{s}_z = 1$, i.e. the nonprecessing state described by the single matrix $R^{(0)}(\hat{n}, \theta_0)$, or $\hat{l}_z = 1$ which corresponds to the HPD state described by the single matrix $R^{(p)}(\hat{n}, \theta_0)$. Both matrices are parametrized by the axis $\hat{n}$ of rotation by the magic angle $\cos\theta_0 = -1/4$ of rotation, which is fixed by the dipole energy. At the interface between these regions $\hat{n} \parallel \vec{H}$: it is the only way to match the precessing $\hat{n}$ on the HPD side with the stationary $\hat{n}$ on the NPD side. According to Eq.(8) this interface is positioned within the counterflow region at the place where $\frac{5}{4}\chi\omega(\omega - H) = \frac{1}{2}\rho_a(\vec{v}_s - \vec{v}_n)^2$, and within the vortex cluster at the place where $\frac{5}{4}\chi\omega(\omega - H) = \lambda_{\text{vortices}}$.

Since F_ω orients the $\hat{n}$ vector perpendicular to magnetic field well inside the HPD region, and $F_{\text{counterflow}}$ or F_{vortices} orients $\hat{l}$ perpendicular to magnetic field deep inside the NPD, which corresponds to $n_z^2 = 1/5$, the $\hat{n}$ texture appears on both sides of the interface. To find the texture one should minimize the orientation energy on each side of the interface together with the gradient energy F_g using the boundary condition $\hat{n} \parallel \vec{H}$ at the interface. In the geometry when the phase boundary is perpendicular to $\vec{H}$ F_g has the same form in terms of the $\hat{n}$ vector for both textures:

$$F_g = \chi c_\perp^2(1-\cos\theta_0)(\partial_i\hat{n})^2 - \frac{1}{2}\chi(c_\perp^2 - c_\parallel^2)(\sin\theta_0\vec{\nabla}\cdot\hat{n} + (1-\cos\theta_0)\hat{n}\cdot\vec{\nabla}\times\hat{n})^2 \quad , \quad (9)$$

where $c_\parallel$ and $c_\perp$ are longitudinal and transverse spin wave velocities (these are related to the Fomin definition[6]: $c_{\parallel\text{Fomin}}^2 = c_\perp^2$ and $c_{\perp\text{Fomin}}^2 = (1/2)(c_\perp^2 + c_\parallel^2)$).

The texture on the HPD side (Fig.3) does not depend on what occurs in the NPD region and coincides with that [4]. The NPD texture depends on the type of the orientational energy in Eq.(4). In Fig.3 the $\hat{l}_z$ texture is shown which takes place within the vortex cluster, while the NPD texture in the counterflow region is slightly different due to violation of the axial symmetry by the fixed direction of the counterflow in the transverse plane. Our NPD texture is essentially smoother

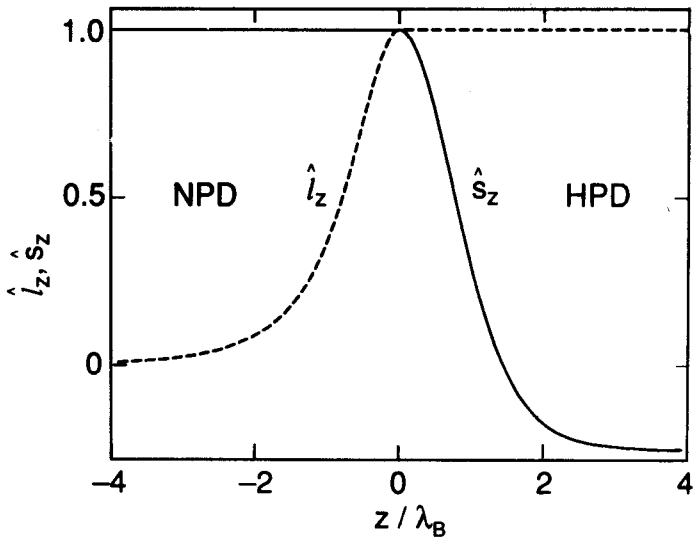

Fig.3. The structure of the HPD-NPD boundary in the presence of vortices or counterflow for particular case $c_\perp = \sqrt{2} c_\parallel$, which holds near T_c. Dashed line – the profile of $\hat{l}_z$, solid line – $\hat{s}_z$. The length is scaled in terms of $\lambda_B = c_\perp / \sqrt{\omega(\omega - H(z_1))} = \sqrt{3/u}\ c_\perp / \Omega_L$, introduced [4].

than that [4], where the gradient energy on the NPD side was not taken into account. At $0 < u < u_c$ both $\hat{n}$ textures, which together comprise the core of the phase boundary between HPD and NPD, have internal thickness $\sim u^{-1/2} c_\perp / \Omega_L$ which diverges at $u \to 0$: at $u = 0$ the thickness of HPD-NPD domain boundary is determined by the magnitude of the magnetic field gradient.[1]

So far experiments were concentrated in the region of small w, where only the HPD-NPD boundary was investigated, and we suggest to extend the region of w to observe the other domain boundaries.

We wish to thank Yu. M. Bunkov, V.V. Dmitriev, M. Krusius, T. Sh. Misirpashaev, and E. Thuneberg for discussions. This work has been supported through the ROTA co-operation project between the Academy of Finland and the USSR Academy of Sciences.

---

1. A. Borovik-Romanov, Yu. Bunkov, V. Dmitriev, and Yu. Mukharsky, Pisma Zh. Eksp. Teor. Fiz. **40**, 256 (1984); [JETP Letters, **40**, (1984)]; I.A. Fomin, Pisma Zh. Eksp. Teor. Fiz. **40**, 260 (1984); [JETP Letters, **40**, (1984)].

2. Yu.M. Bunkov and P.J. Hakonen, J. Low. Temp. Phys. **83**, 323 (1991).

3. Y. Kondo, J.S. Korhonen, M. Krusius et al., Phys. Rev. Lett. **67**, 81 (1991).

4. Yu. Bunkov and O. Timofeevskaya, Pisma Zh. Eksp. Teor. Fiz. **54**, 232 (1991); [JETP Letters, **54**, (1991)].

5. P.J. Hakonen, M. Krusius, M.M. Salomaa et al., J. Low Temp. Phys. **76**, 225 (1989).

6. I.A. Fomin, in Modern Problems in Condensed Matter Sciences, Vol. 26, Helium Three, W.P. Halperin and L.P. Pitaevskii, eds., (North-Holland, 1990), p.610.